

## Anomalous Sinking of Spheres due to Local Fluidization of Apparently Fixed Powder Beds

Jun Oshitani,<sup>1,\*</sup> Toshiki Sasaki,<sup>1</sup> Takuya Tsuji,<sup>2</sup> Kyohei Higashida,<sup>2</sup> and Derek Y. C. Chan<sup>3,4,†</sup>

<sup>1</sup>*Department of Applied Chemistry, Okayama University, Okayama 700-8530, Japan*

<sup>2</sup>*Department of Mechanical Engineering, Osaka University, 2-1 Yamadaoka Suita, Osaka 565-0871, Japan*

<sup>3</sup>*School of Mathematics and Statistics, University of Melbourne, Parkville 3010, Australia*

<sup>4</sup>*Department of Chemistry and Biotechnology, Swinburne University of Technology, Hawthorn 3122, Australia*

(Received 20 October 2015; published 11 February 2016)

The sinking of an intruder sphere into a powder bed in the apparently fixed bed regime exhibits complex behavior in the sinking rate and the final depth when the sphere density is close to the powder bed density. Evidence is adduced that the intruder sphere locally fluidizes the apparently fixed powder bed, allowing the formation of voids and percolation bubbles that facilitates spheres to sink slower but deeper than expected. By adjusting the air injection rate and the sphere-to-powder bed density ratio, this phenomenon provides the basis of a sensitive large particle separation mechanism.

DOI: 10.1103/PhysRevLett.116.068001

The dynamic behavior of continuously agitated granular media has been a subject of interest since the time of Faraday [1], who observed large scale circulating patterns in the granular material that was subjected to steady vibration. Such patterns were quantified more than a century later by magnetic resonance imaging [2]. Furthermore, in a mixed granular system under steady vibration, the larger components were observed to migrate upwards against gravity—the Brazil nut effect [3–10]. Although the general explanation for this phenomenon was that as all the granular components rise and fall, large particles are, on average, transported upwards as the small particles fall into the empty space beneath them. However, detailed investigations revealed that ambient air pressure and particle density differences could cause the larger species to rise or even fall [11]. Indeed, the rise time of an initially submerged large particle exhibited a maximum when the particle density was comparable to the bed density and the rise time was also a function of the air pressure [12].

The above complex effects of particle density and the role of air pressure provide motivation to examine another type of continuously, but much more gently agitated, granular system in which the high energy requirements of maintaining a steady vibration is replaced by air being driven continuously into the bottom of the powder bed. Such air fluidized systems are common in mixing, catalysis, combustion, drying, and granulation applications [13]. As a function of the readily controllable air injection rate, the properties of dry powder beds can change abruptly from solidlike to fluidlike. In fact, the differential segregation of large particles in fully fluidized powder beds has been used as a sustainable method of large particle sorting because the powder bed is fully recyclable [14,15]. Studies of fluidized powder beds have been focused exclusively in the fully

fluidized regime, whereas powder beds in a solidlike regime that prevail at low air injection rates have received little attention [16,17].

Here, we report observations of an unusual density dependence in the sinking rate and the final penetration depth of an intruder sphere in a powder bed under well-controlled air injection conditions where the powder bed is in the apparently fixed bed regime. We adduce evidence to support local fluidization as a mechanism responsible for this phenomenon whereby an understanding of such behavior can underpin the development of a density chromatography method of segregating a large particle based on small differences in the particle densities.

*Experimental.*—Sphere sinking experiments into a powder bed of dry hydrophobic glass beads (diam, 0.21–0.25 mm) held in a cylindrical container were conducted in an apparatus illustrated in Fig. 1. A light, inextensible string connected the sphere via a pulley system to a small counterweight outside the cylinder. The position of the counterweight, measured on a scale attached to the exterior of the container, was used to monitor the changing depth of the sinking sphere in the opaque powder bed. The density of the large hollow plastic intruder sphere was adjusted by filling it with iron or lead powder, with due account of the small mass of the counterweight. The initial sphere position was set manually via the pulley and counterweight system so that the sphere was just in contact with the top of the bed. The counterweight was then released from rest and the motion of the counterweight and the state of the top of the powder bed were recorded by two video cameras. The sphere position and the sinking rate were extracted from these video recordings (see the Supplemental Material [18] for details).

An air distribution system at the bottom of the container ensured uniform air injection [18]. The known rate of air

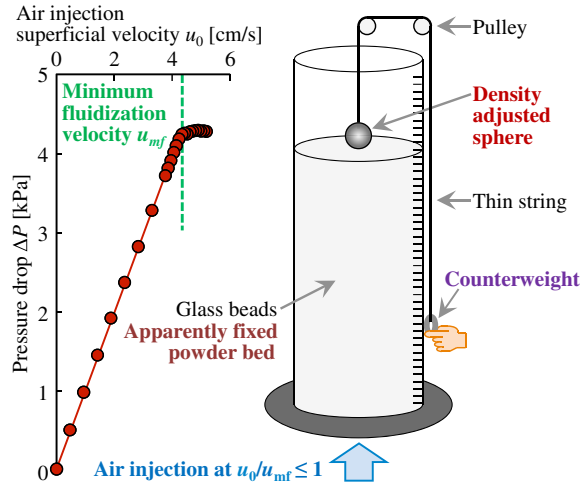


FIG. 1. Measured pressure drop,  $\Delta P$ , as a function of the air injection superficial velocity,  $u_0$  (volumetric rate/container cross-sectional area). The minimum fluidization velocity,  $u_{mf}$ , marks the transition between the linear pressure variation of the apparently fixed bed regime and the constant pressure fluidized powder bed regime. Sphere sinking experiments were conducted at around  $u_0/u_{mf} \sim 1$ . Schematic of the apparatus used to measure the sinking of a sphere ( $D_{\text{sphere}} = 30$  mm) in a cylindrical container (diam, 150 mm) filled to a height of 300 or 150 mm with glass beads (diam, 0.21–0.25 mm) at the powder bed density  $\rho_{\text{bed}} = 1.53$  g/cm<sup>3</sup>; see Ref. [18] for details.

injection was characterized by the air superficial velocity,  $u_0$ . For a small  $u_0$ , the measured pressure drop along the bed column followed the linear Darcy law of fluid transport through a homogeneous rigid porous medium (see Fig. 1). Throughout this linear regime, the bed height remained at the initial static value and the bed surface was quiescent [18]. This is termed the *apparently fixed* bed regime.

When  $u_0$  exceeded the minimum fluidization velocity,  $u_{mf}$ , the pressure drop remained constant (see Fig. 1) as the bed height expanded by up to 10% beyond the static value. Air bubbles could also be seen to percolate continuously from the bed surface. This is termed the *fluidized* powder bed regime [16,17]. To ensure experimental reproducibility, the powder bed was prepared to the same initial steady state [18] before each experimental run.

**Results.**—We first examine results obtained at an air injection superficial velocity of  $u_0/u_{mf} = 0.95$  into a 300 mm deep powder bed. In Fig. 2(a), we show the time variation of the depth,  $h$ , scaled by the sphere diameter,  $D_{\text{sphere}}$  (30 mm), of the sinking spheres of selected densities in the range  $0.85 \leq \rho_{\text{sphere}}/\rho_{\text{bed}} \leq 2.61$ . The vertical scale for  $h$  increases downwards. At  $u_0/u_{mf} = 0.95$ , the powder bed was nominally in the apparently fixed bed regime in which the pressure drop,  $\Delta P$ , vs the superficial velocity,  $u_0$ , behavior shown in Fig. 1 suggested the powder bed should behave like a solid porous medium. However, we see in Fig. 2(a) that spheres of all densities in the above range sank into the bed. The rate of sinking and the final depth at

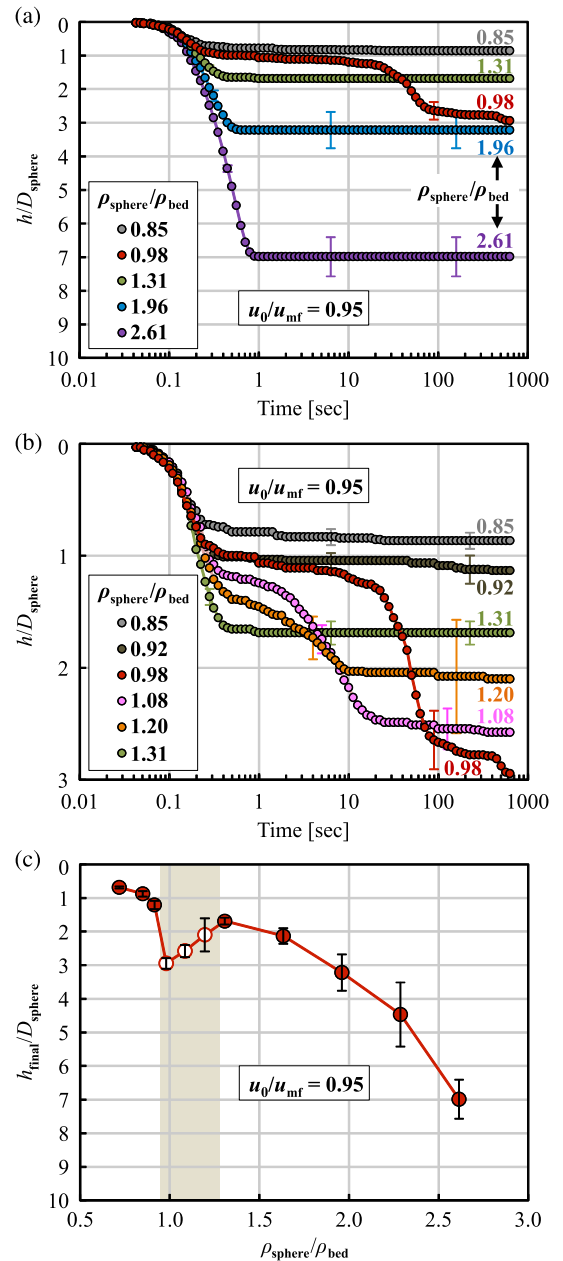


FIG. 2. (a) Variation on a logarithmic time scale of the depth,  $h$ , of sinking spheres scaled by the sphere diameter in the apparently fixed bed regime:  $u_0/u_{mf} = 0.95$  at different sphere densities. See the Supplemental Material [18] for a video visualization of the comparative sinking rate. (b) As in (a), for  $0.85 \leq \rho_{\text{sphere}}/\rho_{\text{bed}} \leq 1.31$ . (c) Variation of the final depth,  $h_{\text{final}}$ , of the sunken sphere with scaled sphere density. The bottom of the 300 mm deep powder bed is at  $h/D_{\text{sphere}} = 10$ . The scale for  $h$  increases downwards.

which the sphere finally came to rest varied with the sphere density,  $\rho_{\text{sphere}}/\rho_{\text{bed}}$ .

The initial rate of sinking appeared to increase with increasing sphere density [see Fig. 2(a)]. However, at density  $\rho_{\text{sphere}}/\rho_{\text{bed}} = 0.98$  the sphere took almost 100

times longer to settle to the final depth. Furthermore, the final depth was deeper than that of a sphere that is  $\sim 30\%$  denser at  $\rho_{\text{sphere}}/\rho_{\text{bed}} = 1.31$ . The sphere with densities close to the bed density,  $0.98 \leq \rho_{\text{sphere}}/\rho_{\text{bed}} \leq 1.20$ , had distinct intermittent variations in the sinking rates [see Fig. 2(b)].

Variation of the final depth of the sphere,  $h_{\text{final}}$ , with sphere density,  $\rho_{\text{sphere}}$ , is shown in Fig. 2(c). The densest sphere,  $\rho_{\text{sphere}}/\rho_{\text{bed}} = 2.61$ , sank to the deepest final depth of  $h_{\text{final}}/D_{\text{sphere}} \sim 7$ . As the sphere density decreased, the final depth also decreased under the expectation that the sinking phenomenon was driven by gravity. However, at  $\rho_{\text{sphere}}/\rho_{\text{bed}} \sim 1.3$ ,  $h_{\text{final}}$  reached a minimum and started to increase with a further decrease in the sphere density [the open symbols in Fig. 2(c)]. This anomaly occurred in the range  $1 < \rho_{\text{sphere}}/\rho_{\text{bed}} < 1.3$  [the shaded region in Fig. 2(c)]. But decreasing the sphere density below  $\rho_{\text{sphere}}/\rho_{\text{bed}} < 1$  resulted in a smaller  $h_{\text{final}}$ . The bottom of the bed was at  $h/D_{\text{sphere}} = 10$ ; thus, this nonmonotonic variation of  $h_{\text{final}}$  with  $\rho_{\text{sphere}}$  was not an effect due to a finite bed depth. Sinking experiments conducted by the same method in a similar powder bed at half the depth (150 mm) showed identical anomalous behavior in the same density range.

We now consider results obtained from varying the air injection superficial velocity into a 150 mm deep powder bed. In Fig. 3(a), we show the final sphere depth scaled by the bed depth,  $h_{\text{final}}/h_{\text{bed}}$ , for  $h_{\text{bed}} = 150$  mm, at different superficial velocities,  $u_0/u_{\text{mf}}$ . These results demonstrate that there is a minimum superficial velocity,  $u_0/u_{\text{mf}} \sim 0.83$ , below which spheres did not sink and the powder bed behaved as a solid. For superficial velocities in the range  $0.83 < u_0/u_{\text{mf}} < 1.0$ , the final sinking depth exhibited a local maximum and minimum as a function of  $\rho_{\text{sphere}}/\rho_{\text{bed}}$  (the open symbols). However, for  $u_0/u_{\text{mf}} > 1.0$ , spheres with  $\rho_{\text{sphere}}/\rho_{\text{bed}} < 1$  did not sink, whereas spheres with  $\rho_{\text{sphere}}/\rho_{\text{bed}} > 1$  did sink.

In Fig. 3(b), we show the final depth,  $h_{\text{final}}$ , as a function of the superficial velocity,  $u_0/u_{\text{mf}}$ , for a sphere of density  $\rho_{\text{sphere}}/\rho_{\text{bed}} = 0.98$ . This demonstrates the general phenomenon that when the sphere density  $\rho_{\text{sphere}}/\rho_{\text{bed}} \sim 1$ , the air injection superficial velocity can be used as a parameter for selective separation of intruder spheres. Indeed, the combination of (i) the different sinking rate of spheres with relative density  $\rho_{\text{sphere}}/\rho_{\text{bed}} \sim 1$  [see Fig. 2(b)], (ii) the time taken to settle down to its final depth [see Figs. 2(a) and 2(c)] and (iii) the sensitivity of the float or sink behavior to variations in  $u_0/u_{\text{mf}}$  [see Fig. 3(a)] can be exploited for targeted large particle separation according to their densities.

By examining the state of the surface of the powder bed as the intruder particle sinks, we can gain some insight into the observed sinking behavior around the parameter space:  $\rho_{\text{sphere}}/\rho_{\text{bed}} \sim 1$  and  $u_0/u_{\text{mf}} \sim 1$ . A set of photos of the powder bed surface that corresponds to the experiments in

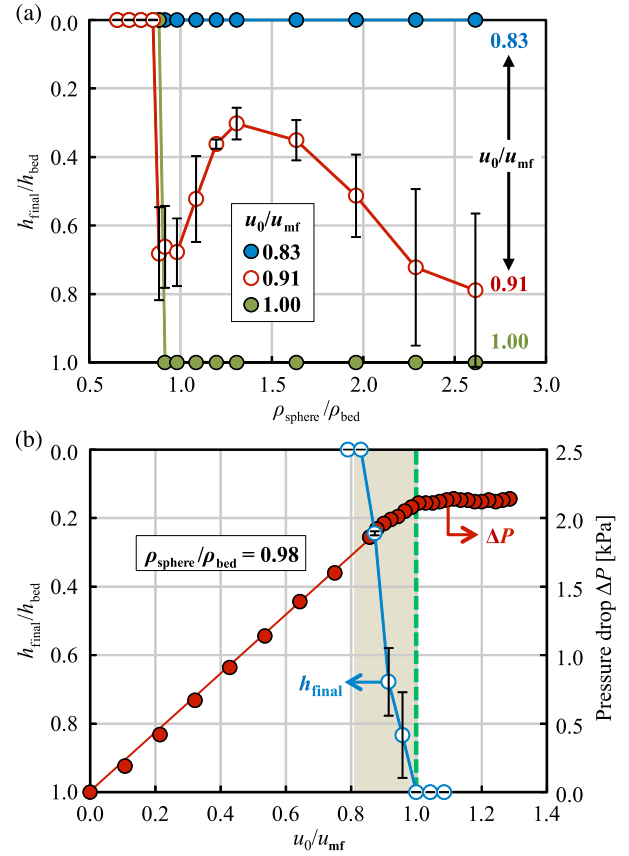


FIG. 3. (a) Variation of the final depth,  $h_{\text{final}}$ , of a sunken sphere scaled by the bed depth,  $h_{\text{bed}}$ , with a sphere density,  $\rho_{\text{sphere}}/\rho_{\text{bed}}$ , at three superficial velocities at or just below  $u_0/u_{\text{mf}} = 1$ , in the apparently fixed bed regime. (b) Variation of the final depth,  $h_{\text{final}}$ , of the sunken sphere (the open symbols, left-hand axis) and the pressure drop,  $\Delta P$  (the solid symbols, right-hand axis), with superficial velocity,  $u_0/u_{\text{mf}}$ , at sphere density  $\rho_{\text{sphere}}/\rho_{\text{bed}} = 0.98$ . The powder bed depth is 150 mm.

Fig. 2(c) at  $u_0/u_{\text{mf}} = 0.95$  are shown in Fig. 4. We note that when  $\rho_{\text{sphere}}/\rho_{\text{bed}} < 1.31$ , bubbles are observed to percolate from the powder bed surface at the location of the sinking sphere, whereas for  $\rho_{\text{sphere}}/\rho_{\text{bed}} \geq 1.31$ , such percolation bubbles are not present. Corresponding video is available in the Supplemental Material [18].

For  $u_0/u_{\text{mf}} < 1$ , the linear relation between the pressure drop,  $\Delta P$ , and the superficial velocity,  $u_0$  (see Fig. 1), means that the powder bed appears to be a fixed bed with a Darcy law permeability that characterizes air transport through the bed.

The reason why spheres with densities well above the powder bed density, e.g., for  $\rho_{\text{sphere}}/\rho_{\text{bed}} > 1.5$  [see Fig. 2(a)], sink in the apparently fixed bed is easier to understand. The inclusion of an impermeable intruder sphere indicates the presence of a local barrier to air flow—the rising air stream has to flow around the bottom of the sphere. If the superficial velocity,  $u_0$ , is below but close to the minimum fluidization velocity,  $u_{\text{mf}}$ , the local air

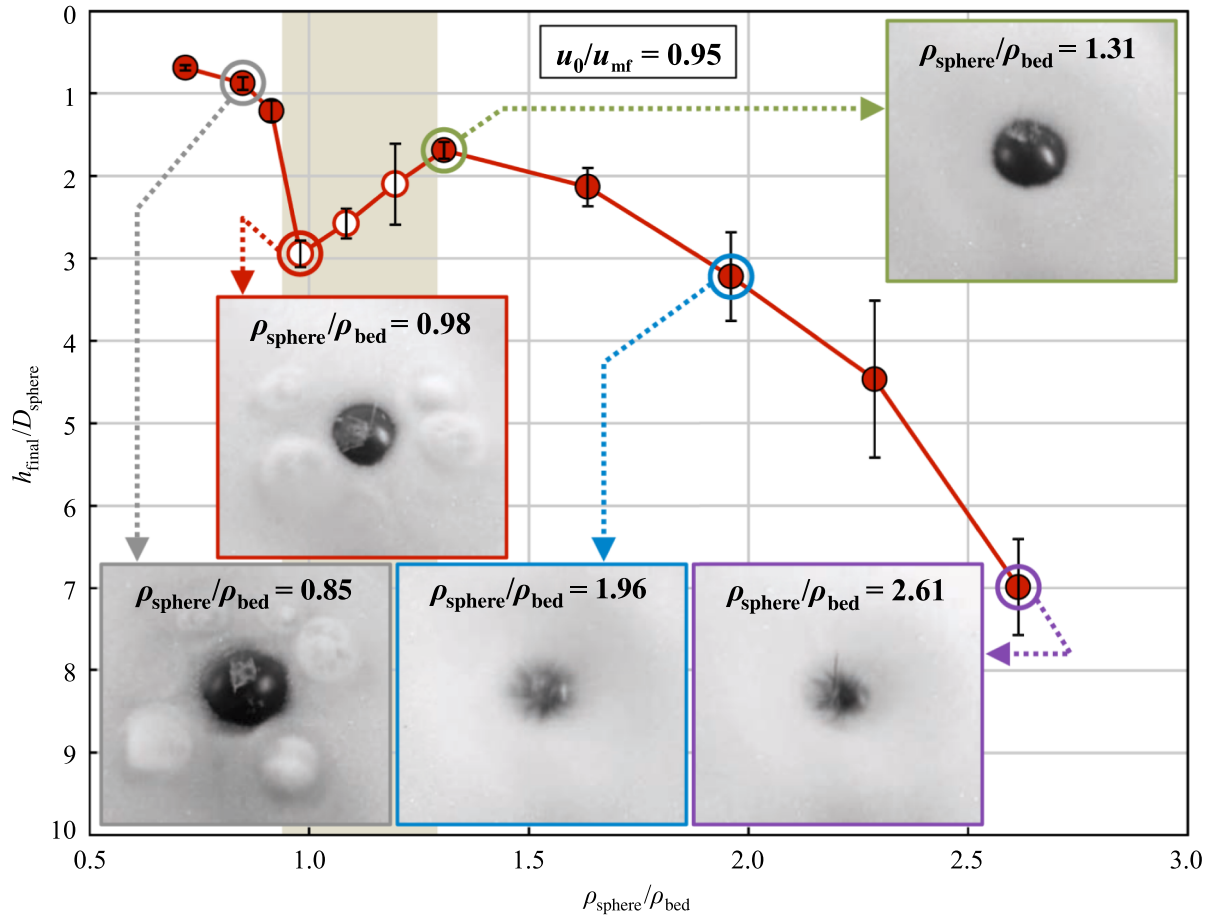


FIG. 4. Photos of the surface of the powder bed as spheres of different densities begin to sink in the experiments depicted in Fig. 2(c). See the Supplemental Material for corresponding videos [18].

flow loosens the structure of the powder bed under the sphere relative to the fixed, rigid powder bed. The looser powder bed structure can facilitate the entrainment of the powder underneath the sphere, allowing powder to be conveyed upwards. This thus allows the sphere to sink. As the sphere sinks deeper, the local powder bed pressure, similar to the hydrostatic pressure due to the weight of the powder bed above that location, will increase until such a point that the powder cannot be convected around the sphere, in spite of its presence as a local barrier to air flow. At this point, the sphere will sink no further. This is also in accord with the observation that the final depth decreases as the sphere density  $\rho_{\text{sphere}}/\rho_{\text{bed}}$  decreases from 2.6 to 1.3.

The appearance of percolation bubbles for  $\rho_{\text{sphere}}/\rho_{\text{bed}} < 1.3$  can be understood as follows. If the sphere density is not high enough, the rising air stream can also lift the light intruder sphere and the local air velocity can cause *local fluidization* around the sphere. As a result, air voids can then form underneath the sphere and migrate to the powder bed surface where they are observed as emerging percolation bubbles.

As the sphere density  $\rho_{\text{sphere}}/\rho_{\text{bed}}$  decreases from 1.3 to 1, the decreasing weight of the sphere allows larger regions of local fluidization to develop. This creates larger voids that allow the sphere to sink deeper in spite of the decreasing sphere density.

When the sphere density,  $\rho_{\text{sphere}}/\rho_{\text{bed}}$ , falls below 1, buoyancy due to the rising air will support the intruder sphere so that it can no longer sink very deep—as we can observe in Fig. 2(c).

Thus for a sphere to sink in the apparently fixed powder bed regime,  $u_0/u_{\text{mf}} < 1$ , the part of the powder bed below the sphere must become looser or be locally fluidized. When  $\rho_{\text{sphere}}/\rho_{\text{bed}} \rightarrow 1$  from above, the local air velocity can exceed the minimum fluidization velocity,  $u_{\text{mf}}$ , accompanied by the appearance of percolation bubbles at the powder bed surface.

*Conclusions.*—We have presented experimental observations of how an intruder sphere with varying density sinks in a powder bed at  $u_0/u_{\text{mf}} < 1$ . This is a hitherto unexplored regime in which the powder bed is normally thought of as being in the rigid or fixed bed state. A qualitative explanation has been advanced for the

nonmonotonic behavior of the final depth of the sinking sphere as a function of sphere density around the powder bed density.

At present, fluidized beds operating at  $u_0/u_{mf} \sim 1.5$  to 2.5 are used to separate mixtures of large particles with two densities on an industrial scale [15]. Here, we demonstrate that at a low air injection superficial velocity  $u_0/u_{mf} \leq 1$  that requires less energy expenditure, the sinking of an intruder particle has a very sensitive dependence on relative density around  $\rho_{\text{sphere}}/\rho_{\text{bed}} \sim 1$ . This offers potential for developing a novel particle separation process by exploiting the combination of a different rate of sinking and the final sunken depth even when differences in the particle densities are small.

As with the well-studied Brazil nut effect associated with vibrated granular systems, the observations reported here for an apparently fixed powder bed will benefit from more detailed experimental investigations. The use of high resolution real time magnetic resonance imaging, a computerized tomography scan, or high speed x-ray imaging [19] can potentially shed light on local dynamic structures of the opaque powder bed. Computer simulation studies may also be used to elucidate the mechanism of the intermittent sinking rate at  $\rho_{\text{sphere}}/\rho_{\text{bed}} \sim 1$ .

This work was supported in part by the Australian Research Council through a Discovery Project Grant to D. Y. C. C.

---

\*oshitani@okayama-u.ac.jp

†D.Chan@unimelb.edu.au

[1] M. Faraday, *Phil. Trans. R. Soc. London* **121**, 299 (1831).

- [2] E. E. Ehrichs, H. M. Jaeger, G. S. Karczmar, J. B. Knight, V. Y. Kuperman, and S. R. Nagel, *Science* **267**, 1632 (1995).
- [3] R. L. Brown, *J. Inst. Fuel* **13**, 15 (1939).
- [4] J. C. Williams, *Powder Technol.* **15**, 245 (1976).
- [5] C. Harwood, *Powder Technol.* **16**, 51 (1977).
- [6] A. Rosato, K. J. Strandburg, F. Prinz, and R. H. Swendsen, *Phys. Rev. Lett.* **58**, 1038 (1987).
- [7] R. Jullien, P. Meakin, and A. Pavlovitch, *Phys. Rev. Lett.* **69**, 640 (1992).
- [8] J. Duran, J. Rajchenbach, and E. Clement, *Phys. Rev. Lett.* **70**, 2431 (1993).
- [9] J. B. Knight, H. M. Jaeger, and S. R. Nagel, *Phys. Rev. Lett.* **70**, 3728 (1993).
- [10] H. M. Jaeger, S. R. Nagel, and R. P. Behringer, *Rev. Mod. Phys.* **68**, 1259 (1996).
- [11] X. Yan, Q. Shi, M. Hou, K. Lu, and C. K. Chan, *Phys. Rev. Lett.* **91**, 014302 (2003).
- [12] M. E. Möbius, B. E. Lauderdale, S. R. Nagel, and H. M. Jaeger, *Nature (London)* **414**, 270 (2001).
- [13] D. Kunii and O. Levenspiel, *Fluidization Engineering*, 2nd ed. (Butterworth, Boston, 1991).
- [14] M. Yoshida, S. Nakatsukasa, M. Nanba, K. Gotoh, T. Zushi, Y. Kubo, and J. Oshitani, *Adv. Powder Technol.* **21**, 69 (2010).
- [15] J. Oshitani, T. Kawahito, M. Yoshita, K. Gotoh, and G. V. Franks, *Minerals engineering* **24**, 70 (2011).
- [16] D. Geldart, *Powder Technol.* **7**, 285 (1973).
- [17] R. G. Holdich, *Fundamentals of Particle Technology* (Midland Information Technology & Publishing, Shepshed, England, 2002).
- [18] See Supplemental Material at <http://link.aps.org/supplemental/10.1103/PhysRevLett.116.068001> for experimental details, additional results and supplementary videos.
- [19] T. Homan, R. Mudde, D. Lohse, and D. van der Meer, *J. Fluid Mech.* **777**, 690 (2015).